Supplemental Figure S1-S7

POLD2 Affects Genomic Stability and Epigenetic Regulation in *Arabidopsis*

Jixiang Zhang[1], Shaojun Xie[2, 3], Jinkui Cheng[1], Jinsheng Lai[4], Jian-Kang Zhu[2, 3], and Zhizhong Gong [1, 5]

[1]State Key Laboratory of Plant Physiology and Biochemistry, College of Biological Sciences, China Agricultural University, Beijing 100193, China.

[2]Shanghai Center for Plant Stress Biology, Shanghai Institutes for Biological Sciences, Chinese Academy of Sciences, Shanghai 200032, China

[3]Department of Horticulture and Landscape Architecture, Purdue University, West Lafayette, IN 47906, USA.

[4] State Key Laboratory of Agrobiotechnology, China National Maize Improvement Center, Department of Plant Genetics and Breeding, China Agricultural University, Beijing 100193, China.

[5]Corresponding author:

Zhizhong Gong

State Key Laboratory of Plant Physiology and Biochemistry, College of Biological Sciences, China Agricultural University, Beijing 100193, China.

Email: gongzz@cau.edu.cn; Tel: 86-10-62733733

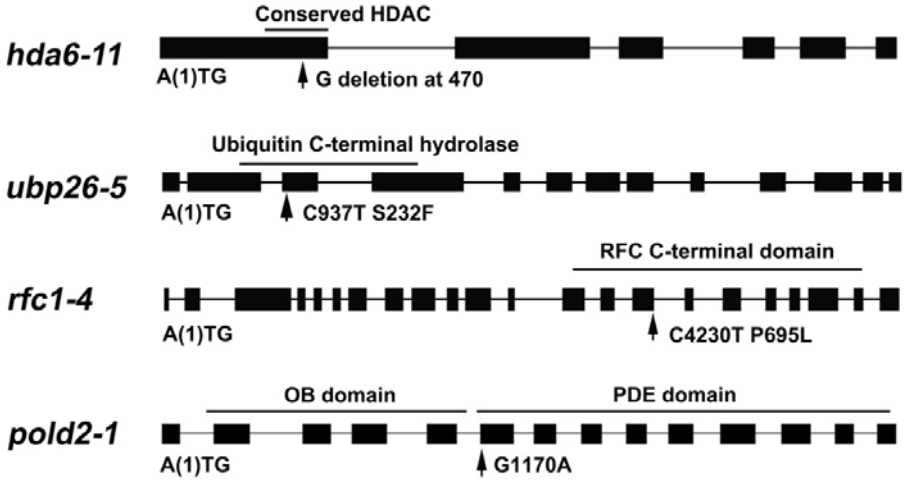

Supplementary Figure S1. Diagrams of *hda6-11*, *ubp26-5*, *rfc1-4*, and *pold2-1* mutations. The positions of exons (solid boxes), introns, and the mutation site are shown.

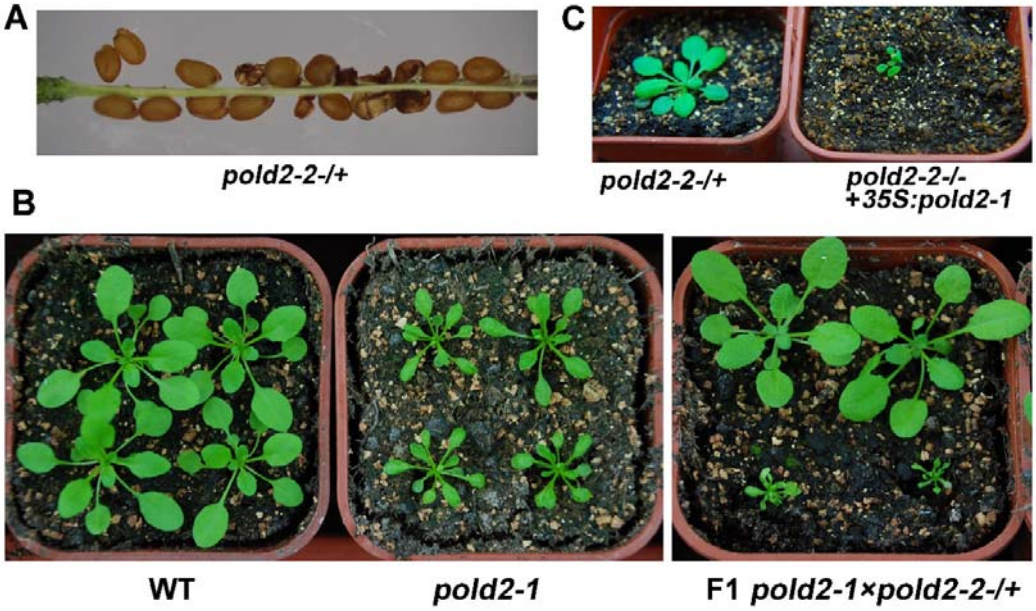

Supplementary Figure S2. Genetic analysis of *pold2-1* with *pold2-2*.

A. *pold2-2* knock out allele caused embryo lethal. Phenotype of a heterozygote *pold2-2* silique; about one-quarter of the heterozygote *pold2-2* seeds were embryo lethal.

B. *pold2-1* and *pold2-2* are allelic. Phenotype of the wild type, *pold2-1*, and F1 of *pold2-1*×*pold2-2-/+*.

C. The mutated cDNA caused by *pold2-1* is partially functional. Phenotype of heterozygote *pold2-2* and homozygote *pold2-2* transformed with mutated *pold2-1* cDNA (the 6-bp deletion transcript).

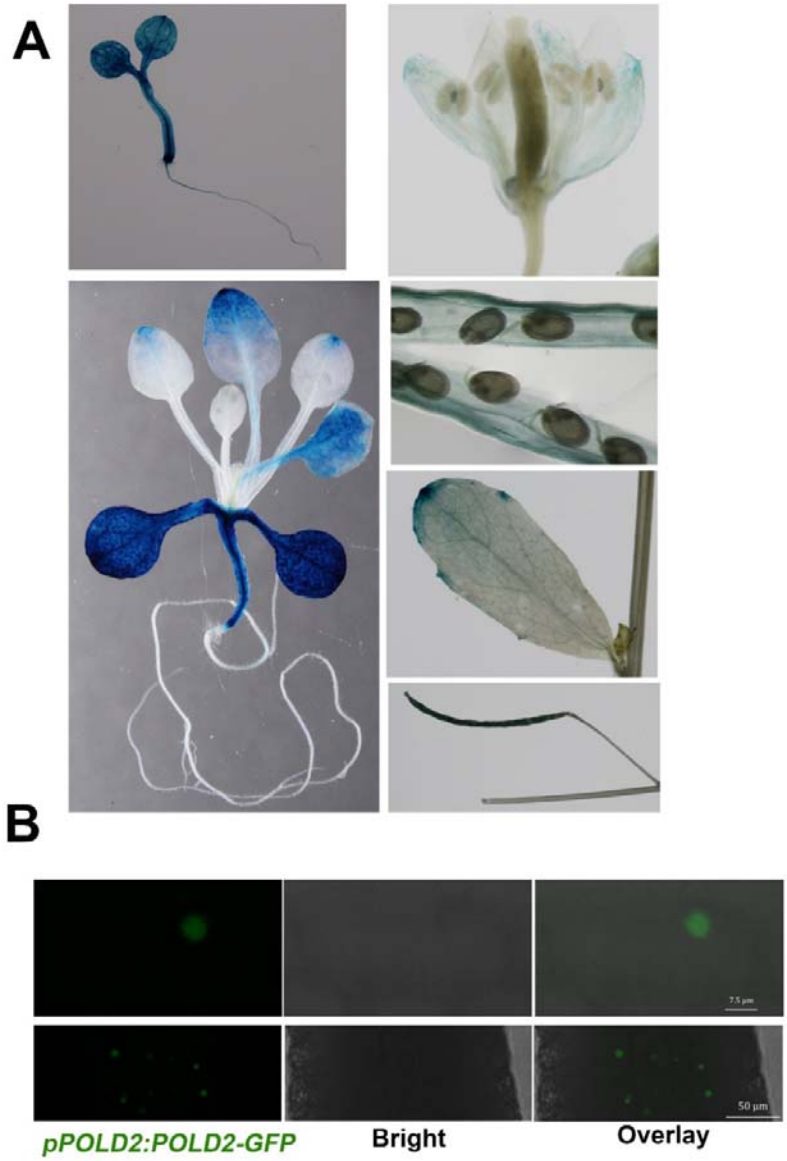

Supplementary Figure S3. POLD2 is a nuclear protein and is ubiquitously expressed.

A. Expression pattern of *ProPOLD2:GUS*. GUS staining in transgenic plants at different stages and carrying *ProPOLD2:GUS*.

B. Subcellular localization of POLD2–GFP fusion protein. The POLD2–GFP signal in 3-day-old seedlings of T2 progeny was imaged with a confocal laser scanning microscope; bar = 7.5 μm (upper) and 50 μm (lower).

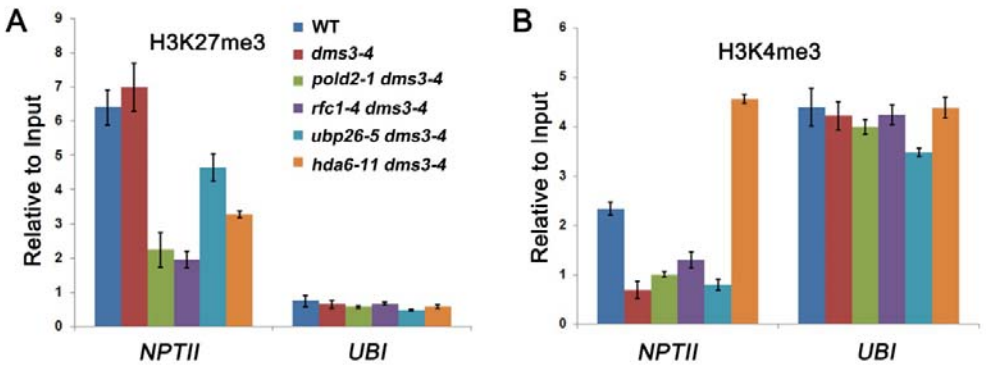

45

46 **Supplementary Figure S4. ChIP-qPCR in *rfc1-4*, *ubp26-5* and *hda6-11* samples.**

47 A. ChIP-PCR to check H3K27me3 level among samples isolated from the same

48 screening. The H3K27me3 level on the *NPTII* was decreased in *pold2-1*, *rfc1-4*,

49 *ubp26-5* and *hda6-11* mutants. *UBI* was a control with lower H3K27me3.

50 B. ChIP-PCR to check H3K4me3 level among samples isolated from the same

51 screening. Comparing to the wild type, H3K4me3 level was decreased in the *dms3-4*

52 mutant but partially restored by *pold2-1*, *rfc1-4*, and *ubp26-5* mutant. *HDA6* mutation

53 greatly increased H3K4me3 on the *NPTII* locus. *UBI* harboring H3K4me3 was used

54 as a control.

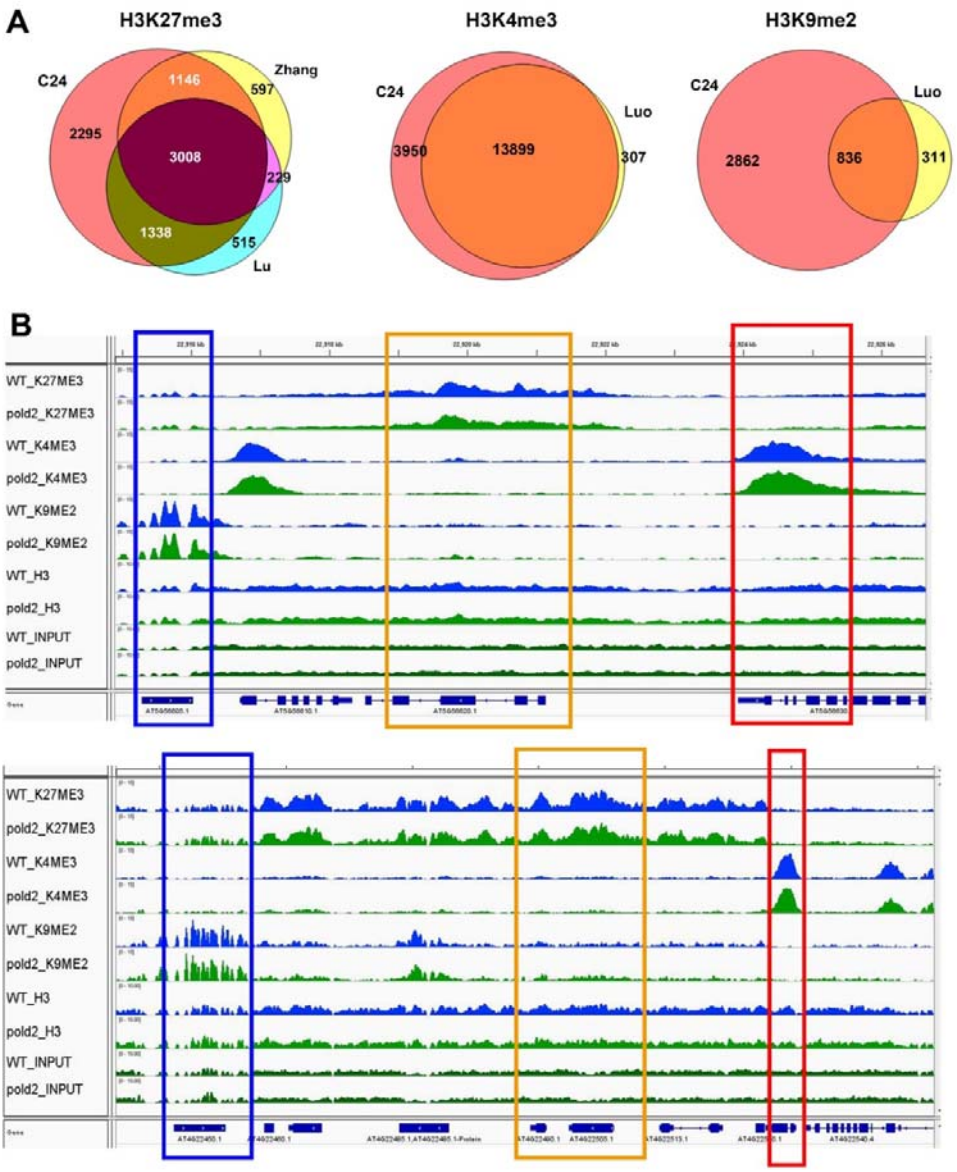

Supplementary Figure S5. Validation of ChIP-seq data.

A. Overlap of histone modification genes identified in this study and in previous studies. Venn diagram of H3K27me3 peaks (left), H3K4me3 peaks (middle), and H3K9me2 peaks (right) in the wild type (C24) in this study demonstrate substantial overlap with previous data from Zhang et al. (1), Lu et al. (2), and Luo et al.(3).

B. Snapshot of selected ChIP-seq data. IGV views of selected reads density (RPKM) of H3K27me3, H3K4me3, H3K9me2, H3, and Input from ChIP-seq data in the wild type (WT) and the *pold2-1* mutant. Blue boxes indicate transposon element (TE) regions harbor H3K9me2. Yellow boxes indicate genes with H3K27me3 modification. Red boxes indicate genes that harbor H3K4me3 modification.

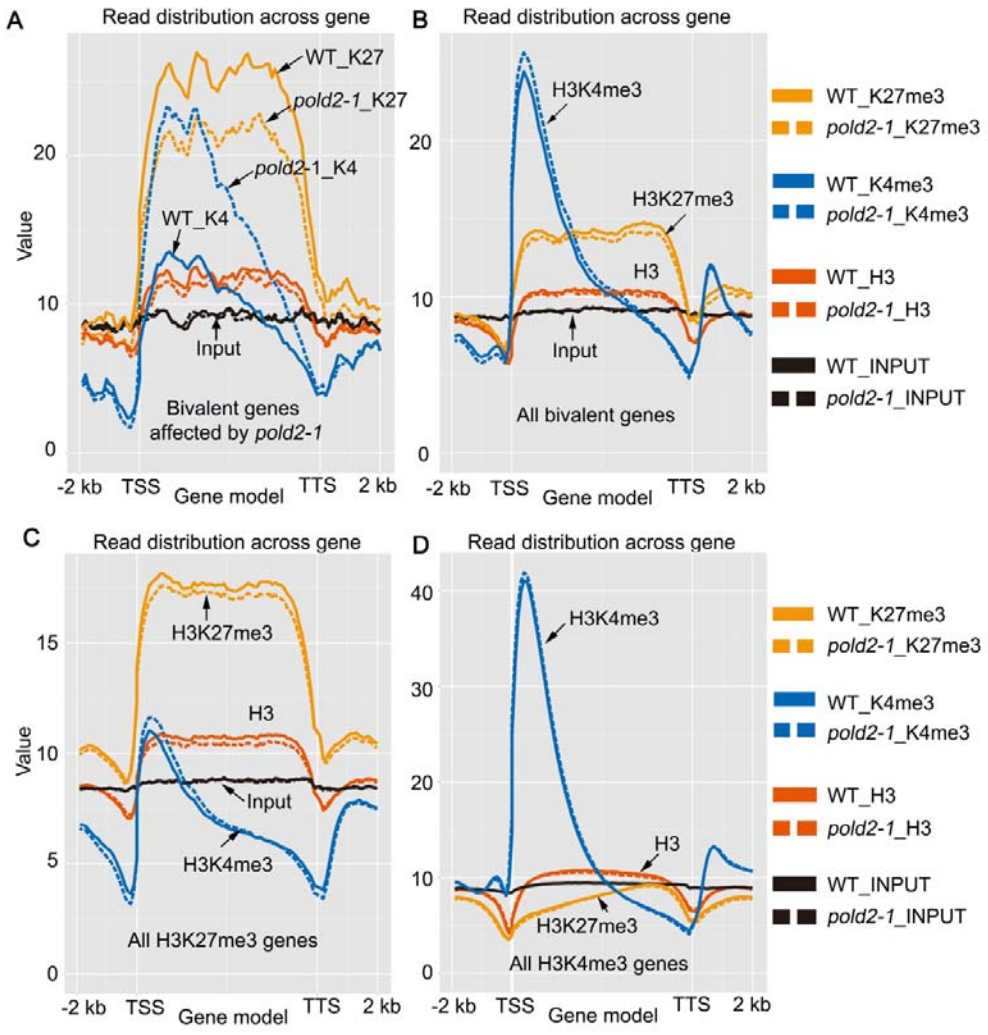

Supplementary Figure S6. Epigenetic profile of bivalent genes affected by *pold2-1* mutant.

A. Altered histone modification profiles of 107 bivalent genes affected by *pold2-1*. Genes were aligned from the transcriptional start sites (TSS) to the transcriptional termination sites (TTS) and divided into 60 bins. The 2,000-bp (2-kb) regions either upstream of TSS or downstream TTS were also included and divided into 20 bins respectively. Histone modification levels of each bin are plotted. *POLD2* mutation results a decrease in H3K27me3 and an increase in H3K4me3 among these 107 bivalent genes.

Epigenetic profile of all bivalent genes (B), all H3K27me3 genes (C), and all H3K4me3 genes (D) was drawn between the wild type (WT) and the *pold2-1* mutant. The level of H3K4me3 and H3K27me3 of these three classes was comparable between WT and *pold2-1* mutant.

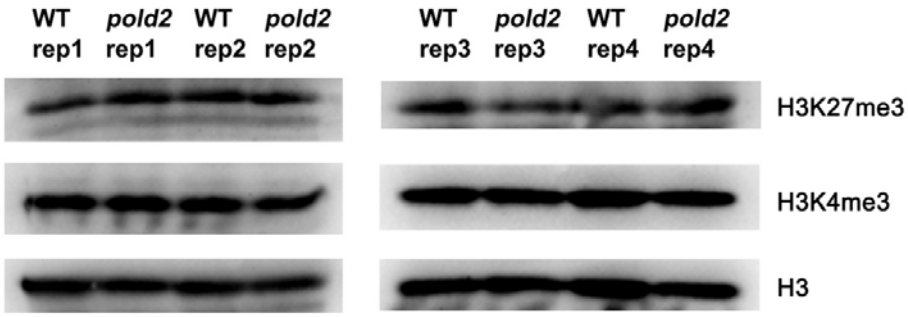

Supplemental Figure S7. Western blot to check global H3K27me3 and H3K4me3 in the *pold2-1* mutant.

Total protein was extracted using 3×SDS extraction buffer (180 mM Tris-HCl pH 6.8, 6% SDS, 30% glycerol, and 15% 2-mercaptoethanol). Proteins were run on a 12% SDS-PAGE for Western blot. Antibodies used were as followed: Anti-H3K27me3 (Ab6002, Abcam, 1:2500 dilution), Anti-H3K4me3 (ab8580, Abcam, 1:5000), Anti-H3 (ab1791, Abcam, 1:5000). Two independent experiments were carried out, each with two biological replicates.

Literature Cited

1. Zhang, X., Bernatavichute, Y.V., Cokus, S., Pellegrini, M. and Jacobsen, S.E. (2009) Genome-wide analysis of mono-, di- and trimethylation of histone H3 lysine 4 in Arabidopsis thaliana. *Genome biology*, **10**, R62.
2. Lu, F., Cui, X., Zhang, S., Jenuwein, T. and Cao, X. (2011) Arabidopsis REF6 is a histone H3 lysine 27 demethylase. *Nat Genet*, **43**, 715-719.
3. Luo, C., Sidote, D.J., Zhang, Y., Kerstetter, R.A., Michael, T.P. and Lam, E. (2012) Integrative analysis of chromatin states in Arabidopsis identified potential regulatory mechanisms for natural antisense transcript production. *Plant J*.